Revised manuscipt tracked Click here to view linked References

FGFR blockade by pemigatinib treats naïve and castration resistant prostate cancer

Paola Chiodelli[1], Daniela Coltrini[1], Marta Turati[1], Marianna Cerasuolo[2], Federica Maccarinelli[1], Sara Rezzola[1], Elisabetta Grillo[1], Arianna Giacomini[1], Sara Taranto[1], Silvia Mussi[1], Alessia Ligresti[3], Marco Presta[1] and Roberto Ronca[1].

[1] University of Brescia, Department of Molecular and Translational Medicine, Brescia, Italy

[2] University of Portsmouth, School of Mathematics and Physics, Hampshire PO1 3HF, UK

[3] National Research Council of Italy, Institute of Biomolecular Chemistry, Pozzuoli, Italy

Running Title: Pemigatinib in the treatment of prostate cancer.

Keywords: FGFR inhibitor, pemigatinib, prostate cancer, castrate resistant prostate cancer, TRAMP, mathematical model.

Correspondence to: Roberto Ronca, University of Brescia, viale Europa 11, 25123 Brescia, Italy. Tel +39-0303717735, FAX +39-0303717747. Email: roberto.ronca@unibs.it

Highlights:

- FGFR inhibition fosters intracellular stress in prostate cancer cells
- Pemigatinib impairs the growth of naïve prostate cancer in vitro and in vivo
- Combination of pemigatinib and enzalutamide leads to long term control of CRPC
- Pemigatinib should be considered for the treatment of PCa and CRPC

ABSTRACT

Prostate cancer (PCa) is a leading cause of cancer mortality in the male population commonly treated with androgen deprivation therapy (ADT) and relapsing as aggressive and androgen-independent castration-resistant prostate cancer (CRPC). In PCa the FGF/FGFR family of growth factors and receptors represents a relevant mediator of cancer growth, tumor-stroma interaction, and a driver of resistance and relapse to ADT.

In the present work, we validate the therapeutic efficacy the FDA-approved FGFR inhibitor pemigatinib, in an integrated platform consisting of human and murine PCa cells, and the transgenic multistage TRAMP model of PCa that recapitulates both androgen-dependent and CRPC settings. Our results show for the first time that pemigatinib causes intracellular stress and cell death in PCa cells and prevents tumor growth in vivo and in the multistage model. In addition, the combination of pemigatinib with enzalutamide resulted in long-lasting tumor inhibition and prevention of CRPC relapse in TRAMP mice. These data are confirmed by the implementation of a stochastic mathematical model and *in silico* simulation.

Pemigatinib represents a promising FDA-approved FGFR inhibitor for the treatment of PCa and CRPC alone and in combination with enzalutamide.

1. INTRODUCTION

Representing the second most frequent tumor in the male population, prostate cancer (PCa) is a leading cause of morbidity and mortality in men, with 1.3 million new cases diagnosed in 2018 and 26,120 estimated deaths in the United States in 2016 [1]. At clinical level, a wide range of prostate lesions exist, with different clinical behaviors ranging from premalignant lesions to very aggressive lethal cancers [2].

Treatment options for PCa are mainly represented by anti-androgen drugs combined or not with prostatectomy and/or radiation therapy. Androgen receptor (AR) signalling plays a central role in PCa, androgen deprivation therapy (ADT) representing the first line of treatment for the advanced disease. However, after a preliminary (12 to 24 months) response to ADT, tumors will eventually progress to an androgen-independent stage termed as castration-resistant prostate cancer (CRPC) with poor prognosis and an average survival of 2-3 years [3]. Different molecular mechanisms are responsible for the acquisition of this hormone refractory phenotype, including continuous activation of the AR axis [4, 5], characterized also by a limited response to chemotherapy and radiotherapy [6, 7]. Thus, effective alternative therapeutic approaches for the treatment of PCa are required.

The fibroblast growth factor (FGF) family members exert their activity by binding to tyrosine kinase FGF receptors (FGFRs), which are expressed by four distinct *FGFR1-4* genes [8]. Experimental and clinical data point to a non-redundant autocrine/paracrine role of the FGF/FGFR system in growth, vascularization and progression of different tumors [9, 10]. In particular, the FGF/FGFR system has been described as an active player in PCa, able to mediate the complex cross-talk between tumor and stroma compartments, and to sustain the transition towards an hormone-refractory state through the deregulation of FGFR signalling by activating mutations or ligand/receptor overexpression [4, 11-16].

Different FGF family members, including FGF2 and FGF8b, are expressed by prostate tumors and play significant paracrine/autocrine functions on cancer epithelial/stromal cells. Aberrant expression of FGFR1 has been reported in epithelial prostate carcinoma cells, and the FGF/FGFR axis has been shown to be active in various stromal components (fibroblasts, endothelial cells, immune infiltrate) associated with PCa cells [4, 17-19]. Recently, a “double negative” molecular subtype of prostate cancer, devoid of AR and neuroendocrine markers expression, has been described emerging after ADT [20]. Interestingly, in this tumor subtype the tumor cells independence from AR is driven by an active MAPK and FGF signaling pathway [20].

Notwithstanding a plethora of non-selective and selective tyrosine kinase FGFR inhibitors have entered the preclinical and clinical assessment [10, 21], only two of them have been approved so far by FDA [22]. Pemigatinib (INCB054828) is a selective and orally available FGFR1-3 inhibitor

endowed with a favourable safety profile and target inhibition [23]. Currently, pemigatinib is approved by the FDA for the second line treatment of patients with cholangiocarcinoma harboring FGFR2 fusions or rearrangements [24, 25], and is under evaluation in phase II clinical trials for patients with urothelial carcinoma, cholangiocarcinoma, and 8p11 myeloproliferative syndrome [23]. Nowadays, complex and integrated models and platforms exist to evaluate the potential of new drug candidates in androgen-dependent and androgen-independent/refractory regimens [26].

In this work we demonstrate that pemigatinib exerts a promising anti-tumor effect on human and murine PCa models *in vitro*, *in vivo*, and in a multistage transgenic model of PCa (TRAMP mice). In addition, *in vivo* experiments and *in silico* simulation using mathematical modelling allowed to confirm not only the *in vivo* efficacy of pemigatinib as a favorable therapy for the treatment of CRPC refractory to second-generation ADT, but also to forecast a long lasting capacity of pemigatinib *plus* enzalutamide to control CRPC relapse and growth.

2. MATERIALS AND METHODS

2.1 Cell lines and reagents. Murine prostate adenocarcinoma TRAMP-C2 cells were obtained from ATCC-LGC Standards Repository (ATCC number CRL-2731) and maintained in DMEM supplemented with 10% heat-inactivated FCS, 10 mmol/L HEPES Buffer, 0.5 mmol/L 2-mercaptoethanol, 2.0 mmol/L glutamine, 5 mg/L bovine insulin, and 10 nmol/L DHT. Enzalutamide-resistant TRAMP-C2 cell line was generated as described in [26]. Human prostate cancer LNCaP (ATCC CRL-1740), DU145 (ATCC HTB-81) and PC3 (ATCC CRL-1435) cells were grown in RPMI 1640 supplemented with 10% FCS. Cells were kept at low passage, returning to original frozen stocks every 3 to 4 months, and tested regularly for Mycoplasma negativity and morphology. Pemigatinib (INCB054828) was provided by Incyte International Sàrl.

2.2 PCR analysis. For mRNA expression analysis, cells were processed, and total RNA was extracted using TRIzol Reagent according to manufacturer's instructions. Contaminating DNA was digested using DNAse and 2.0 μg of total RNA were retro transcribed with MMLV reverse transcriptase using random hexaprimers in a final 20 μL volume. Then, 1/10th of the reaction was analyzed by semiquantitative RT-PCR using specific primers. The PCR products were then electrophoresed on a 1.5% agarose gel and visualized by GelRed staining. Primers used are reported in [27].

2.3 Western Blot analysis. TRAMP-C2 and DU145 were treated for 6 h with pemigatinib and lysed in lysis buffer (TRIS-HCl pH 7 50 mM, NaCl 150mM, Triton X-100 1%, BriJ 0.1%). Protein concentrations were determined using the Bradford protein assay (Bio-Rad Laboratories, Milano, Italy). Then, 40 μg protein/sample were separated by SDS-PAGE, analysed by WB for the

phosphorylated form of FGFRs and $ERK_{1/2}$ (Cell Signaling) and normalized with anti-ERK (Cell Signalling), anti-FGFR1, and anti-GAPDH (Santa Cruz Biotechnology).

2.4 In vitro assays. For details on cell proliferation, clonogenic, soft agar, wound healing, and seahorse assays see Supplementary material section.

2.5 Heterotopic tumor model. Animal experiments were approved by the local animal ethics committee (OPBA, Organismo Preposto al Benessere degli Animali, Università degli Studi di Brescia, Italy) and were performed in accordance with national guidelines and regulations. Eight week-old C57BL/6 or NOD/Scid male mice were injected s.c. with 5 x 10^6 TRAMP-C2 or DU145 cells, respectively. When tumors were palpable (~80mm^3), mice were divided in three groups and treated or not with pemigatinib (0.3 and 1 mg/kg) by daily oral gavage. Tumors were measured in two dimensions and tumor volume was calculated according to the formula $V=(D \times d^2)/2$, where D and d are the major and minor perpendicular tumor diameters, respectively [28]. At the end of the experimental procedure tumors were removed, weighted and processed for histological analyses.

2.6 Seahorse and extracellular flux analyses. Assessment of mitochondrial respiration and glycolytic activity was performed by the Seahorse XFe24 Analyzer (Agilent Technologies) using Seahorse XF Cell Mito Stress Test Kit (Agilent Technologies) according to manufacturer's instructions. Briefly, 4×10^4 cells were seeded on Seahorse XFe24 culture plates (Agilent Technologies) and maintained in complete culture medium for 16 h in the presence of 10 μM pemigatinib or vehicle (DMSO). One hour before the measurement, the medium was changed to Seahorse XF Base Medium supplemented with 2 mM L-glutamine, 1 mM sodium pyruvate and 10 mM glucose and cells were placed in a non-CO_2 incubator. Oxygen consumption rate (OCR) and extracellular acidification rate (ECAR) were measured over time at 6-minutes intervals (2 minutes mixing, 2 minutes recovery, 2 minutes measuring) in a Seahorse XFe24 Extracellular Flux Analyzer (XFe Wave software). Consecutive treatments with oligomycin (1 μM final), 2-[2-[4-(trifluoromethoxy)phenyl]hydrazinylidene]-propanedinitrile (FCCP) (0.5 μM final) and rotenone/antimycin A (0.5 μM final) were performed to enable quantification of basal OCR, ATP-coupled OCR, maximal OCR and spare respiratory capacity. OCR and ECAR were normalized to total cellular protein content determined immediately after each experimental run by Bradford assay.

***2.7 In vivo* experiments with TRAMP mice.** TRAMP mice (C57BL/6-Tg(TRAMP)8247Ng/J) [29] were purchased from The Jackson Laboratory (Bar Harbor, ME, USA), bred crossing homozygous females with C57BL/6J wild type males and heterozygous TRAMP males were used for experimental procedures. Treatment was carried out adding with daily oral gavage of pemigatinib (1 mg/kg) and/or enzalutamide (3 mg/kg) in the drinking water starting from the time indicated in each experiment.

Treated or untreated mice were sacrificed at week 25 of age to collect the genitourinary apparatus that was weighted and prepared for histology.

For prostate histopathological analysis, the genitourinary apparatus was removed from TRAMP male mice, formalin-fixed and paraffin-embedded. Anterior prostate samples were sectioned at a thickness of 7µm, dewaxed, hydrated, and stained with hematoxylin and eosin (H&E) and were evaluated for specific histological abnormalities. The full prostate section was acquired at 20x magnification with a Zeiss Axiovert 200M microscope (Carl Zeiss, Milan, Italy, EU) using the "Mosaic Tool" and the quantification of the pathological areas was performed with the AxioVision LE64 software. Also, the number of pathological adenomeres was determined and pathological areas were graded as described [30].

2.8 Statistical analyses. Statistical analyses were performed using the statistical package Prism 5 (GraphPad Software). Student's *t* test for unpaired data (2-tailed) was used to test the probability of significant differences between two groups of samples. Tumor volume data were statistically analyzed with a 2-way analysis of variance, and individual group comparisons were evaluated by the Bonferroni correction. Differences were considered significant when $p < 0.05$.

3. RESULTS

3.1 Pemigatinib impairs PCa cell growth in vitro

The FGF/FGFR system is actively expressed in various PCa cell lines (Figure S1) and plays relevant roles in the autocrine/paracrine interactions occurring in tumor stroma and parenchyma [9, 16]. As shown in Figure 1A, treatment of prototypical murine (TRAMP-C2) and human (DU145) PCa cells with the FGFR inhibitor pemigatinib efficiently prevented pan-FGFR phosphorylation, leading to decreased activation of the downstream $ERK_{1/2}$ signaling pathway. *In vitro* characterization of the biological impact of pemigatinib on PCa cells revealed that FGFR blockade resulted in a significant inhibition of cell proliferation in both TRAMP-C2 and DU145 cells, with an IC_{50} equal to 2.69 µM and 0.84 µM, respectively (Figure 1B), and induction of apoptosis after 24 hours of treatment with 10 µM of pemigatinib (Figure 1C).

When assessed in a colony formation assay, pemigatinib strongly impaired the clonogenic capacity of both murine and human PCa cells (Figure 1D). Moreover, when tested in a soft agar assay for their resistance to anoikis, pemigatinib significantly reduced the anchorage–independent growth capacity of both TRAMP-C2 and DU145 cells (Figure 1E). Finally, in a wound healing assay, we observed a significant inhibition of the migratory potential of murine and human PCa cells in response to pemigatinib (Figure 1F). Interestingly, the quantification of the repaired area showed a stronger inhibition of cell migration in TRAMP-C2 cells, and resulted in incomplete wound repair in both cell

lines when compared to controls (Figure 1F). These biological observations were extended to other human PCa cell lines (*i.e.* LNCaP and PC3 cells), where pemigatinib efficiently impaired cell proliferation, clonogenic and anchorage-independent growth, and cell migration (Figure S2).

3.2 FGFR blockade by pemigatinib fosters oxidative stress in PCa cells in vitro

Given the recently reported relevant role played by the FGFR pathway in the maintenance of the intracellular redox balance [27], we investigated the intracellular oxidative stress that occurs at cytoplasmic and mitochondrial level after treatment of PCa cells with pemigatinib.

As shown in Figure 2A, treatment with pemigatinib caused a significant increase of cytoplasmic reactive oxygen species (ROS) as detected by the DCFDA probe. In addition, pemigatinib increased mitochondrial ROS (detected by MITOsox probe) and triggered the depolarization of the mitochondrial membrane (detected by TMRE labeling) in both TRAMP-C2 and DU145 cells (Figure 2B-C).

To evaluate the impact of the increased intracellular stress and of the mitochondrial stress/dysfunction, the metabolic profile of TRAMP-C2 and DU145 cells treated with pemigatinib was assessed by the Seahorse Mito Stress Test. As shown in Figure 2D, pemigatinib significantly reduced basal and maximal respiration in both cell lines, as well as ATP production-coupled respiration, expressed as Oxygen Consumption Rate (OCR), without affecting the glycolytic capacity, as assessed by evaluation of the extracellular acidification rate (ECAR).

3.3 Pemigatinib impairs murine and human PCa growth in vivo

Based on the *in vitro* observations, murine TRAMP-C2 and human DU145 cells were grafted s.c. into syngeneic and immunodeficient adult male mice, respectively. When tumors were palpable, tumor bearing animals were treated daily with pemigatinib at 0.3 or 1.0 mg/kg. As shown in Figure 3A-B, tumor growth was significantly reduced in terms of volume and weight by pemigatinib at both doses, with a stronger anti-tumor effect at 1.0 mg/kg. Interestingly, immunohistochemical analysis of harvested tumors confirmed a significant reduction of FGFR activation in pemigatinib-treated samples, that goes along with a reduced cell proliferation (pHH3$^+$) (Figure 3C). In accordance with the oxidative stress observed *in vitro* following treatment with pemigatinib, nitrotyrosine staining revealed an increase of products of tyrosine nitration mediated by reactive nitrogen species in pemigatinib-treated tumors (Figure 3C). Moreover, treatment with pemigatinib led to the formation of necrotic areas in DU145 tumors, as confirmed by H&E staining and TUNEL (Figure 3C).

FGFR1 has been found preferentially expressed in advanced/poorly differentiated tumors in multistage TRAMP model of PCa [31, 32]. Accordingly, prostate-specific conditional ablation of

Fgfr1 in TRAMP mice resulted in the formation of early/well differentiated tumors and was associated with increased survival [33]. On this basis, the promising therapeutic effect exerted by pemigatinib prompted us to assess the impact of this drug in male TRAMP mice until 25 week of age, when well differentiated tumors are present in the prostate lobes and FGF/FGFR play relevant roles [26, 34]. Animals were treated orally with 1.0 mg/kg of pemigatinib starting from week 12, when tumor growth has already started [26, 34], until week 25 and prostate lobes where harvested and examined. As shown in Figure 3D, histopathological analysis revealed a significant reduction of PCa progression in animals treated with pemigatinib when compared with control mice. Indeed, the percentage of pathological areas was reduced from (47.9 ± 4.4)% in untreated mice to (27.6 ± 3.3)% in treated mice. Moreover, the amount of normal/healthy (NH) prostate tissue and of early prostatic intraepithelial neoplasia (PIN) adenomers was significantly increased in TRAMP prostates treated with pemigatinib (Figure 3E-F). Accordingly, and in line with the therapeutic effect of FGFR inhibition, the percentage of well differentiated tumor areas was significantly reduced by pemigatinib (Figure 3E-F).

3.4 Pemigatinib is effective in the treatment of CRPC

Since CRPC represents the most life-threatening setting of PCa, often emerging after first line ADT, we exploited an enzalutamide-resistant TRAMP-C2 cell line obtained after exposition to gradually enriched concentrations of enzalutamide [26].

As shown in Figure 4A, cell proliferation assays were performed on parental and enzalutamide-resistant TRAMP-C2 cells to determine the dose response to pemigatinib. In addition, combination treatments were performed on the two cell lines with increasing concentrations of both pemigatinib and enzalutamide, to determine the potential combinatorial effect of these drugs. The drug combination responses were obtained using the ZIP reference model in SynergyFinder [35] and the results of such analysis are shown in Figure 4B-C. Positive deviations between observed and expected responses imply synergy and are shown in red in the Figure, while negative values denote antagonism and are shown in green. The results point to a promising synergistic anti-tumor effect of the two drugs on both parental and enzalutamide-resistant TRAMP-C2 cells.

On this basis, treatment with pemigatinib was challenged in a CRPC model where TRAMP mice were treated with enzalutamide from week 12 to week 22 to reach the onset of the enzalutamide-resistant state [26]. Under these experimental settings, pemigatinib was added to the treatment schedule from week 22 till week 25 in the absence or in the presence of enzalutamide. As shown in Figure 4D, treatment with pemigatinib alone from week 22 to 25 reduced the pathological areas to (22.4 ± 2.1)%, resulting only in a slight amelioration in respect to enzalutamide alone (31.1 ± 4.9)%.

At variance, the combination regimen (enzalutamide *plus* pemigatinib) from week 22 to 25 significantly blocked tumor progression, resulting in very rare (or no) pathological areas (15.2 ± 3.9)% at the end of the experimental procedure (Figure 4D). The strong impact of pemigatinib on the CRPC state was confirmed by the significant reduction of well differentiated tumor adenomers and increase in healthy (NH) and PIN adenomers observed in tumors treated with pemigatinib or enzalutamide *plus* pemigatinib when compared to enzalutamide alone (Figure 4E-F).

Finally, we implemented and exploited a stochastic mathematical model to predict the long-term response of *in vivo* therapeutic treatments and combinations and explore possible alternative therapeutic settings [26]. To this purpose, combination treatment parameters and data from Figure 4B-C were used for the parametrization of the enriched mathematical model where both the equations of the drug pharmacokinetics, and the interaction between enzalutamide and pemigatinib were considered (details in Supplementary material for the mathematical model and [26]). As shown in Figure 4G-H, *in silico* simulations confirmed the better therapeutic range obtained by the combinatory treatment with enzalutamide *plus* pemigatinib from week 22 to week 25 with respect to the use of pemigatinib or enzalutamide alone. Moreover, long term simulation of the therapeutic effect of combination treatment (Figure 4H) reveals that tumor growth and relapse can be controlled for up to 1 year in the regimen enzalutamide *plus* pemigatinib, thus providing a significant improvement in terms of survival.

4. DISCUSSION

In the era of personalized medicine and of second-line therapies repositioning, old and new targets are emerging as key players in different tumor types. Under this perspective, FGF/FGFR targeting has been gaining increasing interest due to its pleiotropic role in tumor microenvironment and to emerging data reporting its aberrant expression in various tumor types [21, 36-38].

In vitro and *in vivo* observations indicate that the FGF/FGFR system may represent a key mediator in PCa, controlling the progressive independence of epithelial neoplastic cells from stromal cells during tumor evolution [16, 39]. Nevertheless, no FGFR inhibitor has been clinically approved to date for the treatment of PCa, and only one of them (erdafitinib) is under phase II evaluation in PCa patients (NCT03999515) in combination with ADT.

Pemigatinib is a selective tyrosine kinase FGFR1-3 inhibitor recently approved by the FDA for the treatment of metastatic biliary tract cancers harboring FGFR2 fusion or other rearrangement [40] and may represent a promising drug to target FGF/FGFR-driven tumors [9, 10]. In this study we describe for the first time the capacity of pemigatinib to exert a remarkable beneficial therapeutic effect in preclinical models of PCa.

Our data demonstrate that pemigatinib efficiently impairs the proliferative, clonogenic and migratory features of murine and human PCa cell lines. Interestingly, the anti-tumor activity of pemigatinib goes along with an increase in the intracellular oxidative stress and mitochondrial dysfunction, thus resulting in a significant alteration of the metabolic fitness of PCa cells. The involvement of the FGF/FGFR axis in the maintenance of the redox and metabolic equilibrium has recently been reported for other cancer types such as multiple myeloma [41] and lung cancer [27], but never for PCa.
These observations were confirmed i*n vivo*, where treatment with pemigatinib resulted in a significant reduction of the growth of murine and human PCa xenografts in syngeneic and immunodeficient mice, with the appearance of oxidative stress and necrotic areas in the tumor mass. The anti-tumor effect of pemigatinib was confirmed in the multistage murine TRAMP model, where FGFR inhibition led to a significant reduction of tumor burden in the prostate lobes, comparable to the benefit provided by the "state of the art" treatment with the second-generation anti-androgen treatment enzalutamide. ADT represents the first line of PCa treatment, and short or long term tumor relapse represents the rule. "Double negative" PCa, emerging after ADT, is characterized by activated FGFR and MAPK pathways and represents a candidate for the treatment with specific tyrosine kinase inhibitor [20]. Since a consistent number of therapy-refractory patients culminate in more aggressive tumors with neuroendocrine phenotype, the possibility to exploit new therapeutic approaches is crucial for the definition of novel second-line or combination regimens [42]. Relevant to this point, we show for the first time that pemigatinib can provide a relevant and long-lasting benefit for the treatment of the refractory phase of CRPC in the TRAMP model. Indeed, our data prove that the combined treatment of pemigatinib with enzalutamide during the refractory phase of CRPC onset results in a significant reduction of tumor growth, more effective than the treatment with pemigatinib or enzalutamide alone. Accordingly, the implementation of a mathematical model and *in silico* simulation allowed to confirm not only the therapeutic efficacy of the combination enzalutamide *plus* pemigatinib, but also to forecast the capacity of such combination regimen to exert a long lasting maintenance of tumor growth inhibition and the prevention of CRPC relapse.
In a translational perspective few additional considerations should be carried out from this study. First, the proposed model mainly focuses on the upregulation of FGFR and its increased signaling pathway, nevertheless several activating mutations or aberrations in FGFRs have been described in PCa and these might benefit from treatments based on FGFR inhibition as well [16]. In addition, in future studies it would be of great interest and benefit to evaluate if treatment with pemigatinib can improve the efficacy of other clinically relevant AR signaling inhibitors such as abiraterone acetate, apalutamide or darolutamide. Finally, under the safety profile it should be taken into consideration that, given the key role of the FGF axis in "bone biology" [43], the inhibition of the FGF/FGFR axis

arises issues about the alteration of phosphate homeostasis and bone mineralization. Indeed, recent reports suggest the possibility that the inhibition of FGFR results in loss of bone volume in tumor free animals, while it might favour bone volume increase in tumor bearing mice where PCa-bone interactions exist [44, 45]. Even though further and more focused studies are required, these observations suggest that additional benefits of treatment with FGFR inhibitors might be obtained by a proper selection of PCa patients depending on the presence or absence of PCa bone disease/metastases.

In conclusion, pemigatinib represents a promising FDA-approved FGFR inhibitor to be considered for the treatment of PCa and CRPC alone and in combination with enzalutamide.

Acknowledgements. R.R. was supported by Incyte International Sàrl and Associazione Italiana per la Ricerca sul Cancro (AIRC IG 2019 – ID. 23151); M.P. was supported by Associazione Italiana Ricerca sul Cancro (AIRC IG 2019 – ID. 18493); F.M., S.R. and E.G. were supported by a Fondazione Umberto Veronesi (FUV) fellowship.

Conflict of interest disclosure: No conflict to disclose

Author contributions. P.C., D.C., M.T., S.R., E.G., A.G., S.T., S.M. A.L., performed experiments; M.C. performed the statistical and mathematical analyses; R.R: and P.C. conceived and supervised experiments; M.P. and R.R. provided funding; P.C., M.P. and R.R. drafted the manuscript, M.P. and R.R. revised the manuscript.

FIGURE LEGENDS

Figure 1. *In vitro* effect of pemigatinib on PCa cells. A) Western blot analysis of pan-phospho-FGFR, phospho-$ERK_{1/2}$, total FGFR and total ERK in TRAMP-C2 and DU145 cells treated with pemigatinib. GAPDH was used as internal normalization control. B) Cell proliferation of tumor cells treated with increasing doses of pemigatinib for 96 hours was determined by viable cell counting through cytofluorimetric analysis. C) Induction of apoptosis after 24 hours of treatment with pemigatinib determined by quantification of PI and Annexin V positive cells. D) Quantification and representative images of long term colony formation potential after treatment with pemigatinib. E) Anchorage independent growth capacity of TRAMP-C2 and DU145 cells in soft agar. F) Motility of TRAMP-C2 and DU145 cells was assessed quantifying the percentage of repaired area 24 hours after the wound. Representative images of the best treatment conditions are reported. Data are the mean ± SEM, experiments were performed in triplicate. *$p < 0.05$, **$p < 0.01$, ***$p < 0.001$.

Figure 2. Oxidative stress and Seahorse analysis upon treatment with pemigatinib. Tumor cells were treated with 10 μM of pemigatinib and Cytofluorimetric analyses were performed for cytoplasmic (A) or mitochondrial (B) ROS production assessed by DCFDA and MITOsox probes, respectively. C) Under similar conditions the mitochondrial membrane depolarization was determined by TMRE staining. In the plots the red line refers to the gate setting the positive/negative cell population. Data are mean ± SEM. **$p < 0.01$, ***$p < 0.001$. D) Seahorse Mito Stress Test (OCR=oxygen consumption rate, ECAR= extracellular acidification rate) performed on TRAMP-C2 and DU145 cells treated or not with pemigatinib 10 μM. Energy metabolic profile and histograms with the quantification of EACR, basal and maximal OCR, and ATP-linked OCR for both cell lines. Data are mean ± SEM. *$p < 0.05$, **$p < 0.01$, ***$p < 0.001$.

Figure 3. *In vivo* effect of pemigatinib on PCa growth. *In vivo* growth and final weight of subcutaneous TRAMP-C2 (A) and DU145 (B) tumors treated with vehicle or pemigatinib (0.3 or 1 mg/kg) enzalutamide. Data are the mean ± SEM of 8-10 tumors/group. C) Immunohistochemistry of explanted tumors (treated with vehicle or pemigatinib 1mg/kg) and quantification. Scale bar: 100 μm. D) Quantification (percentage) of the pathological area in the anterior prostate of TRAMP mice treated or not with pemigatinib (1 mg/kg). E) Histopathological evaluation of normal healthy (NH, in grey), prostatic intraepithelial neoplasia (PIN, in green) and well differentiated (WD, in white) tumors in the prostate of untreated (NT) or treated TRAMP mice. F) Representative pictures of prostate

adenomers at 12 and 25 weeks (scale bar: 100 μm). Data are the mean ± SEM; n=8 or more animals/group; $*p < 0.05$, $**p < 0.01$, $\#p < 0.0001$.

Figure 4. Effect of pemigatinib in CRCP settings. Cell proliferation assay performed on TRAMP-C2 parental or TRAMP-C2 enzalutamide resistant cells to test pemigatinib alone (A) or the combination of pemigatinib with enzalutamide at different concentrations (B-C). D) Quantification (percentage) of the pathological area in the anterior prostate of TRAMP mice treated under different treatment conditions. Dashed line represents the treatment (mean value) with pemigatinib alone at week 25. E) Histopathological evaluation of normal healthy (NH, in grey), prostatic intraepithelial neoplasia (PIN, in green) and well differentiated (WD, in white) tumors in the prostate of untreated (NT) or treated TRAMP mice. F) Representative pictures of prostate adenomers at 25 weeks (scale bar: 100μm). Data are the mean ± SEM; n= 8 or more animals/group; $*p < 0.05$, $**p < 0.01$, $***p < 0.001$, $\#p < 0.0001$. G-H) Simulation of tumor progression in TRAMP mice treated with enzalutamide from 12W to 22W and pemigatinib from 22W onward (G), or enzalutamide treatment from 12W onward and pemigatinib from 22W onward (H). Dots represents the experimental data and the lines are 30 realizations of the dynamics of enzalutamide-sensitive and -resistant tumor cells in time, described by the stochastic equations (Supplementary material Eq1-6).

Conflict of interest disclosure: No conflict to disclose

REFERENCES

[1] R.L. Siegel, K.D. Miller, A. Jemal, Cancer statistics, 2016, CA. Cancer J. Clin., 66 (2016) 7-30.

[2] P.A. Humphrey, H. Moch, A.L. Cubilla, T.M. Ulbright, V.E. Reuter, The 2016 WHO Classification of Tumours of the Urinary System and Male Genital Organs-Part B: Prostate and Bladder Tumours, European urology, 70 (2016) 106-119.

[3] H. Beltran, T.M. Beer, M.A. Carducci, J. de Bono, M. Gleave, M. Hussain, W.K. Kelly, F. Saad, C. Sternberg, S.T. Tagawa, I.F. Tannock, New therapies for castration-resistant prostate cancer: efficacy and safety, Eur. Urol., 60 (2011) 279-290.

[4] A.C. Hsieh, E.J. Small, C.J. Ryan, Androgen-response elements in hormone-refractory prostate cancer: implications for treatment development, Lancet Oncol, 8 (2007) 933-939.

[5] B.J. Feldman, D. Feldman, The development of androgen-independent prostate cancer, Nat Rev Cancer, 1 (2001) 34-45.

[6] F. Joly, I.F. Tannock, Chemotherapy for patients with hormone-refractory prostate cancer, Ann Oncol, 15 (2004) 1582-1584.

[7] J.E. Damber, G. Aus, Prostate cancer, Lancet, 371 (2008) 1710-1721.

[8] D.E. Johnson, L.T. Williams, Structural and functional diversity in the FGF receptor multigene family. [Review], Advances in Cancer Research, 60 (1993) 1-41.

[9] M. Presta, P. Chiodelli, A. Giacomini, M. Rusnati, R. Ronca, Fibroblast growth factors (FGFs) in cancer: FGF traps as a new therapeutic approach, Pharmacology & therapeutics, 179 (2017) 171-187.

[10] G.C. Ghedini, R. Ronca, M. Presta, A. Giacomini, Future applications of FGF/FGFR inhibitors in cancer, Expert review of anticancer therapy, 18 (2018) 861-872.

[11] K.L. Schwertfeger, Fibroblast growth factors in development and cancer: insights from the mammary and prostate glands, Curr Drug Targets, 10 (2009) 632-644.

[12] V.D. Acevedo, M. Ittmann, D.M. Spencer, Paths of FGFR-driven tumorigenesis, Cell Cycle, 8 (2009) 580-588.

[13] M. Presta, P. Oreste, G. Zoppetti, M. Belleri, E. Tanghetti, D. Leali, C. Urbinati, A. Bugatti, R. Ronca, S. Nicoli, E. Moroni, H. Stabile, M. Camozzi, G.A. Hernandez, S. Mitola, P. Dell'Era, M. Rusnati, D. Ribatti, Antiangiogenic activity of semisynthetic biotechnological heparins: low-molecular-weight-sulfated Escherichia coli K5 polysaccharide derivatives as fibroblast growth factor antagonists, Arteriosclerosis, thrombosis, and vascular biology, 25 (2005) 71-76.

[14] V.D. Acevedo, R.D. Gangula, K.W. Freeman, R. Li, Y. Zhang, F. Wang, G.E. Ayala, L.E. Peterson, M. Ittmann, D.M. Spencer, Inducible FGFR-1 activation leads to irreversible prostate adenocarcinoma and an epithelial-to-mesenchymal transition, Cancer Cell, United States, 2007, pp. 559-571.

[15] S. Memarzadeh, L. Xin, D.J. Mulholland, A. Mansukhani, H. Wu, M.A. Teitell, O.N. Witte, Enhanced paracrine FGF10 expression promotes formation of multifocal prostate adenocarcinoma and an increase in epithelial androgen receptor, Cancer Cell, United States, 2007, pp. 572-585.
[16] A. Giacomini, E. Grillo, S. Rezzola, D. Ribatti, M. Rusnati, R. Ronca, M. Presta, The FGF/FGFR System in the Physiopathology of the Prostate Gland, Physiological reviews, (2020).
[17] K. Maruyama-Takahashi, N. Shimada, T. Imada, Y. Maekawa-Tokuda, T. Ishii, J. Ouchi, H. Kusaka, H. Miyaji, S. Akinaga, A. Tanaka, K. Shitara, A neutralizing anti-fibroblast growth factor (FGF) 8 monoclonal antibody shows anti-tumor activity against FGF8b-expressing LNCaP xenografts in androgen-dependent and -independent conditions, Prostate, 68 (2008) 640-650.
[18] M.M. Mattila, P.L. Harkonen, Role of fibroblast growth factor 8 in growth and progression of hormonal cancer, Cytokine Growth Factor Rev, 18 (2007) 257-266.
[19] R. Ronca, P. Alessi, D. Coltrini, E. Di Salle, A. Giacomini, D. Leali, M. Corsini, M. Belleri, C. Tobia, C. Garlanda, E. Bonomi, R. Tardanico, W. Vermi, M. Presta, Long pentraxin-3 as an epithelial-stromal fibroblast growth factor-targeting inhibitor in prostate cancer, J Pathol, 230 (2013) 228-238.
[20] E.G. Bluemn, I.M. Coleman, J.M. Lucas, R.T. Coleman, S. Hernandez-Lopez, R. Tharakan, D. Bianchi-Frias, R.F. Dumpit, A. Kaipainen, A.N. Corella, Y.C. Yang, M.D. Nyquist, E. Mostaghel, A.C. Hsieh, X. Zhang, E. Corey, L.G. Brown, H.M. Nguyen, K. Pienta, M. Ittmann, M. Schweizer, L.D. True, D. Wise, P.S. Rennie, R.L. Vessella, C. Morrissey, P.S. Nelson, Androgen Receptor Pathway-Independent Prostate Cancer Is Sustained through FGF Signaling, Cancer cell, 32 (2017) 474-489 e476.
[21] M. Katoh, Fibroblast growth factor receptors as treatment targets in clinical oncology, Nature reviews. Clinical oncology, 16 (2019) 105-122.
[22] A. Weaver, J.B. Bossaer, Fibroblast growth factor receptor (FGFR) inhibitors: A review of a novel therapeutic class, Journal of oncology pharmacy practice : official publication of the International Society of Oncology Pharmacy Practitioners, (2020) 1078155220983425.
[23] P.C.C. Liu, H. Koblish, L. Wu, K. Bowman, S. Diamond, D. DiMatteo, Y. Zhang, M. Hansbury, M. Rupar, X. Wen, P. Collier, P. Feldman, R. Klabe, K.A. Burke, M. Soloviev, C. Gardiner, X. He, A. Volgina, M. Covington, B. Ruggeri, R. Wynn, T.C. Burn, P. Scherle, S. Yeleswaram, W. Yao, R. Huber, G. Hollis, INCB054828 (pemigatinib), a potent and selective inhibitor of fibroblast growth factor receptors 1, 2, and 3, displays activity against genetically defined tumor models, PloS one, 15 (2020) e0231877.
[24] G.K. Abou-Alfa, V. Sahai, A. Hollebecque, G. Vaccaro, D. Melisi, R. Al-Rajabi, A.S. Paulson, M.J. Borad, D. Gallinson, A.G. Murphy, D.Y. Oh, E. Dotan, D.V. Catenacci, E. Van Cutsem, T. Ji,

C.F. Lihou, H. Zhen, L. Feliz, A. Vogel, Pemigatinib for previously treated, locally advanced or metastatic cholangiocarcinoma: a multicentre, open-label, phase 2 study, The Lancet. Oncology, 21 (2020) 671-684.
[25] V. Merz, C. Zecchetto, D. Melisi, Pemigatinib, a potent inhibitor of FGFRs for the treatment of cholangiocarcinoma, Future oncology, 17 (2021) 389-402.
[26] M. Cerasuolo, F. Maccarinelli, D. Coltrini, A.M. Mahmoud, V. Marolda, G.C. Ghedini, S. Rezzola, A. Giacomini, L. Triggiani, M. Kostrzewa, R. Verde, D. Paris, D. Melck, M. Presta, A. Ligresti, R. Ronca, Modeling Acquired Resistance to the Second-Generation Androgen Receptor Antagonist Enzalutamide in the TRAMP Model of Prostate Cancer, Cancer research, 80 (2020) 1564-1577.
[27] A. Giacomini, S. Taranto, S. Rezzola, S. Matarazzo, E. Grillo, M. Bugatti, A. Scotuzzi, J. Guerra, M. Di Trani, M. Presta, R. Ronca, Inhibition of the FGF/FGFR System Induces Apoptosis in Lung Cancer Cells via c-Myc Downregulation and Oxidative Stress, International journal of molecular sciences, 21 (2020).
[28] A. Giacomini, S. Matarazzo, K. Pagano, L. Ragona, S. Rezzola, M. Corsini, E. Di Salle, M. Presta, R. Ronca, A long pentraxin-3-derived pentapeptide for the therapy of FGF8b-driven steroid hormone-regulated cancers, Oncotarget, 6 (2015) 13790-13802.
[29] N.M. Greenberg, F. DeMayo, M.J. Finegold, D. Medina, W.D. Tilley, J.O. Aspinall, G.R. Cunha, A.A. Donjacour, R.J. Matusik, J.M. Rosen, Prostate cancer in a transgenic mouse, Proc. Natl. Acad. Sci. U. S. A., 92 (1995) 3439-3443.
[30] S.B. Shappell, G.V. Thomas, R.L. Roberts, R. Herbert, M.M. Ittmann, M.A. Rubin, P.A. Humphrey, J.P. Sundberg, N. Rozengurt, R. Barrios, J.M. Ward, R.D. Cardiff, Prostate pathology of genetically engineered mice: definitions and classification. The consensus report from the Bar Harbor meeting of the Mouse Models of Human Cancer Consortium Prostate Pathology Committee, Cancer Res., 64 (2004) 2270-2305.
[31] W.J. Huss, R.J. Barrios, B.A. Foster, N.M. Greenberg, Differential expression of specific FGF ligand and receptor isoforms during angiogenesis associated with prostate cancer progression, Prostate, 54 (2003) 8-16.
[32] N.M. Greenberg, Transgenic models for prostate cancer research, Urologic oncology, 2 (1996) 119-122.
[33] F. Yang, Y. Zhang, S.J. Ressler, M.M. Ittmann, G.E. Ayala, T.D. Dang, F. Wang, D.R. Rowley, FGFR1 is essential for prostate cancer progression and metastasis, Cancer research, 73 (2013) 3716-3724.

[34] R. Ronca, A. Giacomini, E. Di Salle, D. Coltrini, K. Pagano, L. Ragona, S. Matarazzo, S. Rezzola, D. Maiolo, R. Torrella, E. Moroni, R. Mazzieri, G. Escobar, M. Mor, G. Colombo, M. Presta, Long-Pentraxin 3 Derivative as a Small-Molecule FGF Trap for Cancer Therapy, Cancer cell, 28 (2015) 225-239.
[35] A. Ianevski, A.K. Giri, T. Aittokallio, SynergyFinder 2.0: visual analytics of multi-drug combination synergies, Nucleic acids research, 48 (2020) W488-W493.
[36] T. Helsten, S. Elkin, E. Arthur, B.N. Tomson, J. Carter, R. Kurzrock, The FGFR Landscape in Cancer: Analysis of 4,853 Tumors by Next-Generation Sequencing, Clin Cancer Res, 22 (2016) 259-267.
[37] Y. Tanner, R.P. Grose, Dysregulated FGF signalling in neoplastic disorders, Semin Cell Dev Biol, 53 (2016) 126-135.
[38] A. Giacomini, P. Chiodelli, S. Matarazzo, M. Rusnati, M. Presta, R. Ronca, Blocking the FGF/FGFR system as a "two-compartment" antiangiogenic/antitumor approach in cancer therapy, Pharmacol Res, 107 (2016) 172-185.
[39] G. Yan, Y. Fukabori, G. McBride, S. Nikolaropolous, W.L. McKeehan, Exon switching and activation of stromal and embryonic fibroblast growth factor (FGF)-FGF receptor genes in prostate epithelial cells accompany stromal independence and malignancy, Molecular and cellular biology, 13 (1993) 4513-4522.
[40] A. Rizzo, A.D. Ricci, G. Frega, A. Di Federico, G. Brandi, FGFR inhibitors in elderly patients with advanced biliary tract cancer: an unsolved issue, Expert review of gastroenterology & hepatology, (2021) 1-8.
[41] R. Ronca, G.C. Ghedini, F. Maccarinelli, A. Sacco, S.L. Locatelli, E. Foglio, S. Taranto, E. Grillo, S. Matarazzo, R. Castelli, G. Paganini, V. Desantis, N. Cattane, A. Cattaneo, M. Mor, C. Carlo-Stella, A. Belotti, A.M. Roccaro, M. Presta, A. Giacomini, FGF Trapping Inhibits Multiple Myeloma Growth through c-Myc Degradation-Induced Mitochondrial Oxidative Stress, Cancer research, 80 (2020) 2340-2354.
[42] A. Aparicio, C.J. Logothetis, S.N. Maity, Understanding the lethal variant of prostate cancer: power of examining extremes, Cancer discovery, 1 (2011) 466-468.
[43] N. Su, M. Jin, L. Chen, Role of FGF/FGFR signaling in skeletal development and homeostasis: learning from mouse models, Bone research, 2 (2014) 14003.
[44] E. Labanca, E.S. Vazquez, P.G. Corn, J.M. Roberts, F. Wang, C.J. Logothetis, N.M. Navone, Fibroblast growth factors signaling in bone metastasis, Endocrine-related cancer, 27 (2020) R255-R265.

[45] J.Y. Estefania Labanca, Peter Shepherd, Xinhai Wan, Justin M. Roberts, Michael W. Starbuck and Nora M. Navone, A specific pan-FGFR inhibitor has antitumor activity against prostate cancer patient derived xenografts, PDX, expressing high FGFR1, Cancer research, 78 (2018) 1.

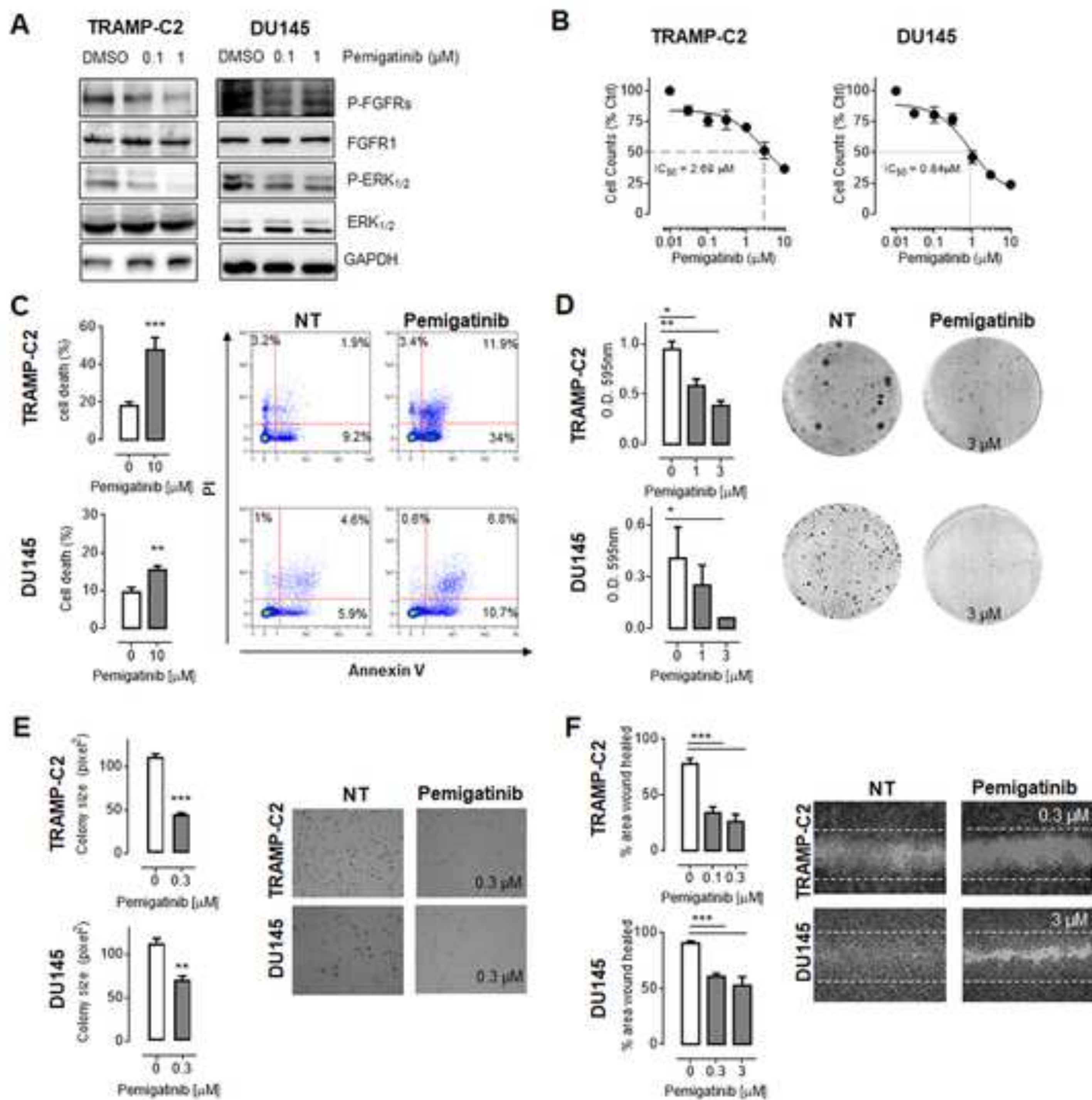
A
TRAMP-C2
DU145
DMSO 0.1 1
DMSO 0.1 1
Pemigatinib (μM)
P-FGFRs
FGFR1
P-ERK1/2
ERK1/2
GAPDH
B
TRAMP-C2
DU145
Cell Counts (% Ctrl)
Pemigatinib (μM)
C
TRAMP-C2
DU145
cell death (%)
Pemigatinib [μM]
NT
Pemigatinib
PI
Annexin V
D
O.D. 595nm
3 μM
E
Colony size (pixel²)
0.3 μM
F
% area wound healed
0.3 μM
3 μM

New Figure 2

Click here to access/download;Figure(s);new Figure 2.tif

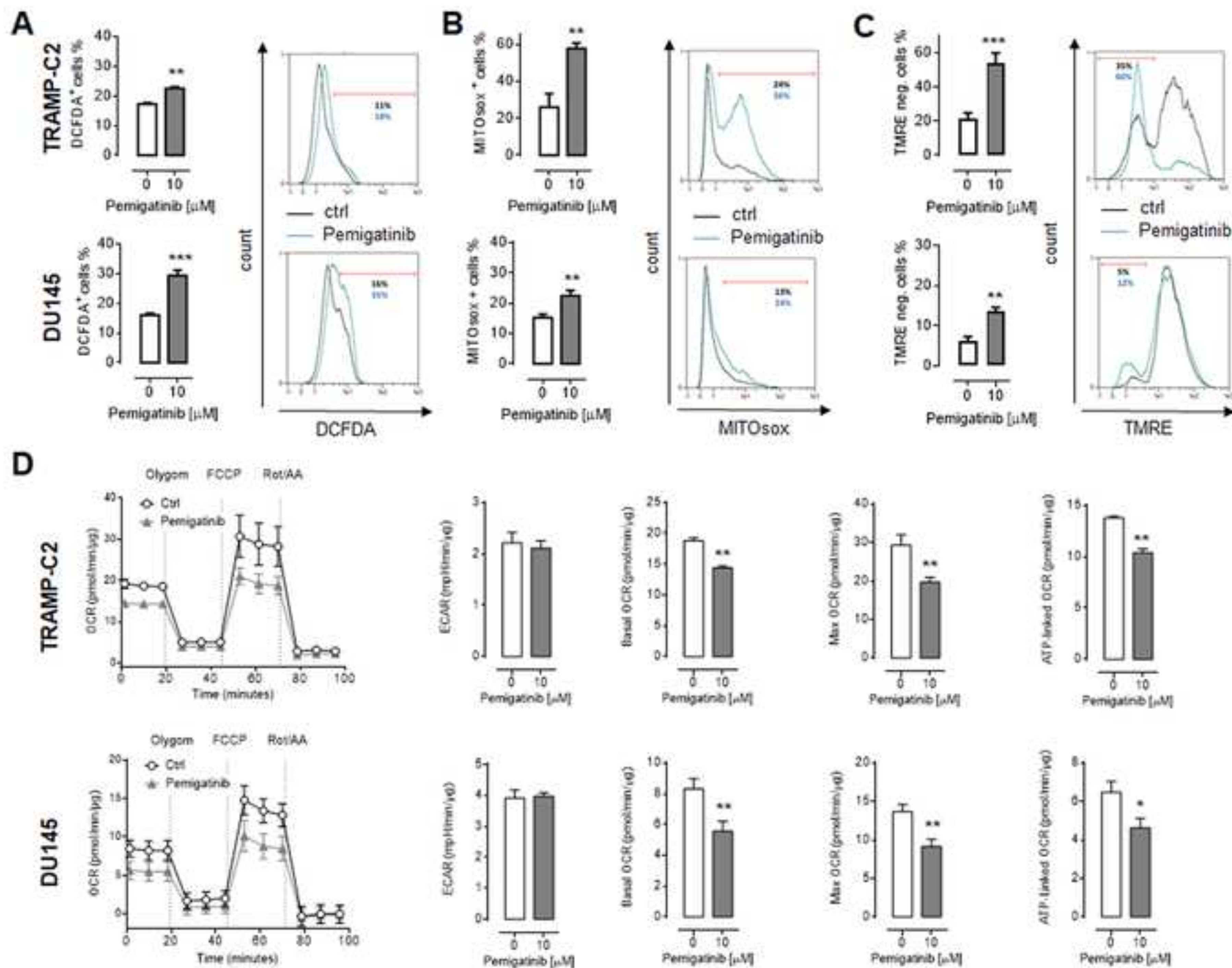

Figure 3

Click here to access/download;Figure(s);Figure 3.tif

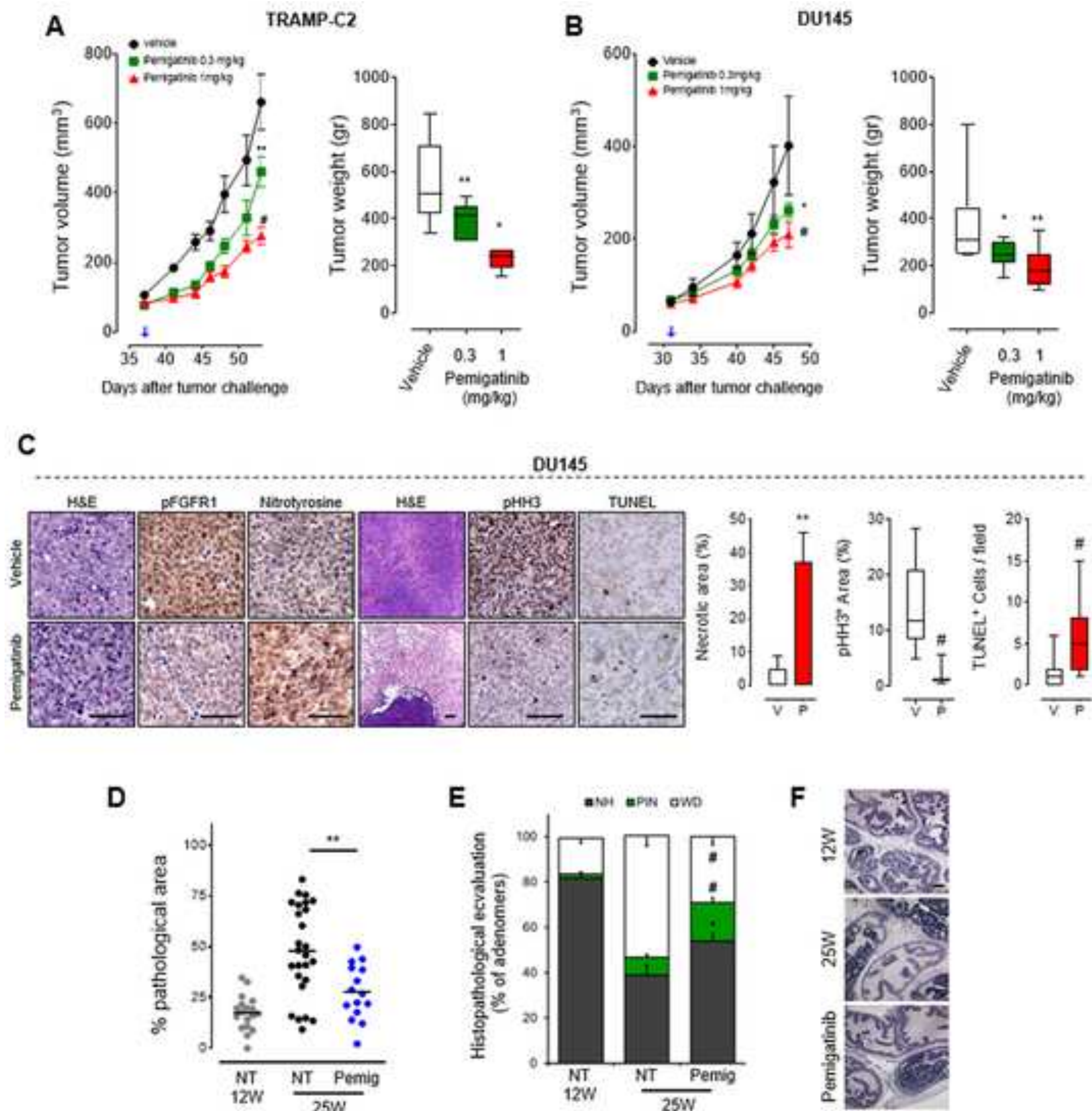

New Figure 4 Click here to access/download;Figure(s);new Figure 4.tif